

Journal of Robotics and Mechanical Engineering Research

An Application of Mathematical Morphology Operators as Features Extraction Method for Low Speed Slew Bearing Condition Monitoring

Wahyu Caesarendra^{1,2}, Dwi B Wibowo¹, Mochammad Ariyanto¹, Joga D Setiawan^{*1}

¹Mechanical Engineering Department, Faculty of Engineering, Diponegoro University, Semarang 50275, Indonesia

²School of Mechanical, Materials and Mechatronic Engineering, University of Wollongong, Wollongong, New South Wales 2522, Australia

***Corresponding author:** Joga D. Setiawan, Ph.D, Mechanical Engineering Department, Faculty of Engineering, Diponegoro University, Semarang, Indonesia; Tel: +62-24-746-0059; Email: joga.setiawan@gmail.com

Article Type: Research, **Submission Date:** 04 September 2015, **Accepted Date:** 06 October 2015, **Published Date:** 27 October 2015.

Citation: Wahyu Caesarendra, Dwi B Wibowo, Mochammad Ariyanto, Joga D Setiawan (2015) An Application of Mathematical Morphology Operators as Features Extraction Method for Low Speed Slew Bearing Condition Monitoring. J Robot Mech Eng Resr 1(3): 1-13.

Copyright: © 2015 Joga D. Setiawan, et al. This is an open-access article distributed under the terms of the Creative Commons Attribution License, which permits unrestricted use, distribution, and reproduction in any medium, provided the original author and source are credited.

Abstract

This paper presents a new application of mathematical morphology (MM) operators for low speed slew bearing condition monitoring. The MM operators were used as a signal processing step and feature extraction method for bearing vibration signals. Four basic MM operators; erosion, dilation, closing and opening, were studied. This paper also investigates another potential MM operator, namely gradient operator. Two common time domain features in bearing condition monitoring, namely root mean square (RMS) and kurtosis, were extracted from the processed signal. The study shows that the changes in bearing condition can be clearly detected from the extracted features (RMS and kurtosis) of the MM operators compared to RMS and kurtosis features extracted from the original vibration signal. The application of the method is demonstrated with laboratory run-to-failure slew bearing data acquired on a daily basis.

Keywords: Feature extraction, Low speed slew bearing, Mathematical morphology operators

Introduction

Slew bearing is a subgroup of rolling element bearings commonly used in large industrial machinery such as turntables, steel mill cranes, offshore cranes, rotatable trolleys, excavators, reclaimers, stackers, swing shovels, and ladle cars. They typically support high axial and high radial load. Slewing bearings are often critical production parts. An unplanned downtime when a bearing breaks down can be very expensive due to the loss of production. Moreover, as replacement of large slew bearings can take several months to arrive due to long manufacturing and delivery times, plants often carry spare bearings to guard against these unforeseen circumstances. In order to prevent unplanned downtime, a condition monitoring and prognosis method is needed [1]. The criteria to replace the bearing to prevent fatal failure in bearing condition monitoring is features. Features can be defined as representative values to indicate bearing conditions. This is because the features are extracted from raw vibration signals acquired from rolling element bearing. The features identifying certain values indicate whether the condition of the

bearing is normal or failing.

The running condition of slew bearings in high load, low rotational speed and reversible rotation, generates a non-linear vibration signal. The non-linear vibration signal is difficult to analyse using conventional vibration analysis such as FFT and time domain feature extraction using mean, RMS, skewness and kurtosis. Hence, a study of the sensitivity of the condition monitoring parameters is required. In addition, the low energy impact due to the contact between defective spots and the rolling element generates a very weak vibration signal which is deeply masked by background noise. When the time domain features are extracted from the vibration signal where the noise is dominant, they are insensitive to any changes in the bearing condition. When the vibration amplitude eventually exceeds the background noise, the feature values do increase significantly but this point serious bearing damage has already occurred and often by this stage, the bearing condition is already close to unsustainable fault.

This paper is an extension of previous studies investigating the appropriate features for low speed slew bearing condition monitoring used in the local steel mill industry [1,2]. The present study, demonstrates a new application of mathematical morphology (MM) operators for low speed slew bearing condition monitoring. The MM operators were used as a signal processing step and feature extraction method for the bearing vibration signal. Four basic MM operators (erosion, dilation, closing and opening) were studied. This paper also presents another potential MM operator, namely gradient operator. Two common features, root mean square and kurtosis, were extracted from the processed signal. The study shows that the changes in the bearing condition can be detected clearly from these features of the MM operators unlike those extracted from the original vibration signal. The application of the method is demonstrated with laboratory run-to-failure slew bearing data acquired on a daily basis.

Mathematical Morphology Method

A Brief Review of Mathematical Morphology Method

Mathematical morphology (MM) was initially introduced as a non-linear image processing method to analyze two dimensional

(2D) image data including binary images and grey-level images based on set theory [3]. The basic principle of the MM method is to modify the shape of the original signal by transforming it through its intersection with another object called the 'structuring element' (SE). Four operators including erosion, dilation, closing and opening are used to achieve the transformation.

After having been applied successfully in 2D image processing, the MM method has been used in biomedical one dimensional (1D) signal analysis for EEG signals [4-6] and ECG signals [7]. The first known study of MM in 1D vibration signals was presented by Nikolaou and Antoniadis [8]. They used the MM method for vibration data with prior knowledge of inner race and outer race faults. The effects of four morphological operators on the enveloping impulse-type signals are examined. The result shows that the 'closing' operator is more suitable for extracting the impulse signal corresponding to the bearing fault type. The SE value was empirically investigated within the range of 0.2T to 1.2T. The optimum SE for a signal with additive noise was selected as 0.6T (0.6 times the pulse repetition period).

The multi-scale morphological analysis was developed by Zhang et al [9]. The method shows independency of empirical rules in terms of SE selection, but the technique is quite complex. The vibration bearing data used in this paper is gathered from open access data from Case Western Reserve. Wang et al [10] proposed an improved morphological filter for the features extraction of periodic impulse signals. An average weighted combination of open-closing and close-opening morphological operators was employed to eliminate the statistical deflection of amplitude and to extract the impulse component from the original signal. To optimize the SE, they used a new criterion called impulse attenuation (IMA). Dong et al [11] presented the fault diagnosis of rolling element bearings using the modified morphological method. The morphological operator used in their method was the average weight combination of the closing and opening operator. They proposed a new criterion called SNR criterion to optimize the length of SE. In this paper, three vibration datasets are collected from three measurements such as rolling element defect, inner race defect and outer race defect. Another recently published research on MM was presented by Santhana Raj and Murali [12]. The authors combined the MM operators with fuzzy inference to classify the bearing faults. The vibration data collected from the artificial bearing defects used in the paper are similar to Zhang et al [9].

The literature [9-12] has demonstrated the effectiveness of the MM application in detecting the bearing fault frequencies from among impulsive-type signals. These signals are generated from known bearing conditions such as inner and/or outer race faults. It has been known that the signals from artificial faults are easier to identify than natural bearing faults and typically, the impulse-type signals are easily identified visually without any additional tool or processing step [11]. In this study, the MM method is applied in naturally damaged slew bearing data. The bearing in this study was running from brand new to failure. Unlike the vibration signal characteristics presented in [9-12], the slew bearing signal has its own characteristic, a non-linear – low amplitude vibration signal which is masked by the background noise. Thus the objective of the MM method is to minimize the background noise and extract the bearing signal. Once the background noise is removed, bearing condition can be clearly identified.

Mathematical Morphology Operators

The original discrete one dimensional (1D) signal and structuring element (SE) have to be first determined to use the four basic

operators in the MM method. Suppose the discrete 1D discrete vibration signal $x = \{x(1), x(2), \dots, x(N)\}$, which functions over a domain $x(n) = (1, 2, \dots, N)$. And let $S = \{S(1), S(2), \dots, S(M)\}$ be the SE, which is the discrete function over a domain $S(m) = (1, 2, \dots, M)$, where N and M are integers and $N \geq M$. Then, the four morphology operators for the discrete 1D vibration signal can be defined as follows:

- *Erosion*: also refer to min filter.

$$(x \ominus S)(n) = \min[x(n+m) - S(m)] \quad (1)$$

- *Dilation*: also refer to max filter.

$$(x \oplus S)(n) = \max[x(n-m) + S(m)] \quad (2)$$

- *Closing*: Dilates 1D signal and then erodes the dilated signal using the same structuring element for both operations.

$$(x \bullet S)(n) = ((x \oplus S) \ominus S)(n) \quad (3)$$

- *Opening*: Erodes 1D signal and then dilates the eroded signal using the same structuring element for both operations.

$$(x \circ S)(n) = ((x \ominus S) \oplus S)(n) \quad (4)$$

where $n \in (1, 2, \dots, N)$ and $m \in (1, 2, \dots, M)$, the notation $\ominus, \oplus, \bullet, \circ$ denote the erosion operator or Minkowski subtraction, dilation operator or Minkowski addition, closing operator and opening operator in the MM method, respectively.

The original simulated 1D signal is shown in Figure 1(a). The illustration of various effects of the basic MM operators applied in the simulated 1D vibration signal are presented in Figure 1(b)-(e). The simulated signal has zero mean value which is typical of 1D vibration signal. The work principle of the basic MM operators can be summarized as follows: erosion of $x(n)$ by the structuring element $A(m)$ reduces the positive part and enlarges the negative part of $x(n)$, while dilation of $x(n)$ by the structuring element $A(m)$ reduces the negative part and enlarges the positive part of $x(n)$. In addition, closing of $x(n)$ smooths the signal $x(n)$ by cutting down any impulses in the negative part and opening $x(n)$ smooths the signal $x(n)$ by cutting down its impulses in the positive part.

Another operator that might be useful is called gradient operator proposed by Santhana Raj and Murali [12]. This operator is also studied in this paper. The two gradients operators are as follows:

- *Gradient 1*: Taking the different between the original 1D signal and the eroded signal.

$$(x \ominus S)(n) - x(n) = x(n) - \min[x(n+m) - S(m)] \quad (5)$$

- *Gradient 2*: Taking the different between the dilated signal and the original 1D signal.

$$(x \oplus S)(n) - x(n) = \max[x(n-m) + S(m)] - x(n) \quad (6)$$

Structuring Element (SE) of the Mathematical Morphology Method

Three properties in the construction of the SE according to Dong et al [11] are the shape, the length (domain), and the height (amplitude). As an important point many studies have been done on the effect of SE on the result.

Selection of the shape of the SE: In MM analysis, the shapes of the SE can vary from regular to irregular curves, such as flat, triangular, semicircular and so on. Zhang et al [9] found that the shapes of the SE have little effect on the analysis. The flat SE is selected in this study to simplify the computation.

The height of the SE: All the heights of the flat SE are defined as zeros with the aim of retaining the shape character of the signal.

Determination of the length of the SE: The length of the SE is

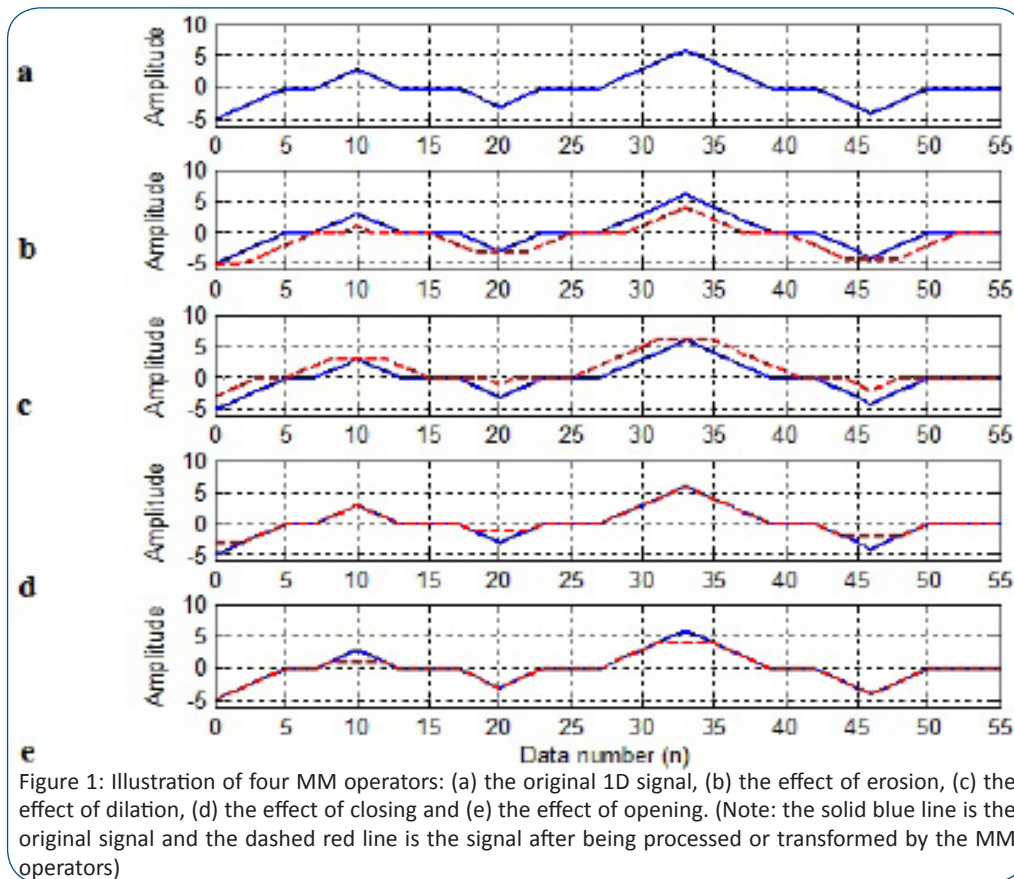


Figure 1: Illustration of four MM operators: (a) the original 1D signal, (b) the effect of erosion, (c) the effect of dilation, (d) the effect of closing and (e) the effect of opening. (Note: the solid blue line is the original signal and the dashed red line is the signal after being processed or transformed by the MM operators)

an important aspect in the MM analysis. The different SE value is also examined within the range of 0.2T to 1.2T and the optimum SE for signals with additive noise is selected as 0.6T (0.6 times the pulse repetition period). In practical applications, to define the optimum SE requires experiments in MM analysis. To illustrate the effects of four basic MM operators in 1D impulse features, assume the selected flat SE is {1,1,1,1}.

Experimental Set-up

The vibration of accelerated wear test data used in this paper was acquired from a laboratory slew bearing test rig as shown in Figure 2. The test rig was operated in continuous rotation at 1 rpm. The slew bearing used was an INA YRT260 type axial/radial bearing supplied by Schaeffler with an inner and outer diameter of 260 mm and 385 mm, respectively. The vibration data was acquired from four accelerometers installed on the inner radial surface at 90 degrees to each other (see Figure 2(b)) with 4880 Hz sampling rates. The accelerometers were IMI608 A11 ICP-type sensors. The accelerometers were connected to a high speed Pico scope DAQ (PS3424). The bearing began running in 2006, however in order to provide continuous monitoring and produce run-to-failure bearing data, the bearing data was collected from February to August 2007 (139 days). In order to accelerate the bearing service life, coal dust was injected into the bearing in mid-April 2007 (58 days from the beginning). In practice, especially in steel making companies, the slew bearing is located in the open air where the bearing is exposed to a dusty environment and for this reason, the coal dust was inserted to simulate the real working conditions.

The schematic of the slew bearing test rig showing the main drive reducer, the hydraulic load and how the bearing is attached is shown in Figure 2(a). The axial load was applied via a hydraulic load of approximately 30 tons.

Results and Discussion

Vibration-based FFT

Initially, vibration-based fast Fourier transformation (FFT) was used to identify the dominant frequencies of the vibration signal. The bearing fault frequencies of the slew bearing when the bearing runs at 1 rpm are presented in Table 1. It has been known that if the FFT of the vibration signal contains one or more dominant frequencies which are identical to or match one of the fault frequencies shown in Table 1, a certain fault type has occurred. The three selections of slew bearing data and their FFT are presented in Figures 3 to 5.

The vibration data and its FFT before dust contamination on February 24 (1st day), one month after dust insertion on May 3 (58th day) and three days before bearing failure on August 30 (138th day) are depicted in Figure 3, Figure 4 and Figure 5, respectively. The FFT result in Figure 3(b) shows that the frequency is less than 100 Hz. After dust insertion, the frequency of the vibration signal is dominated by high frequencies of 1356 Hz, 1770 Hz and 2167 Hz, as shown in Figure 4(b). When the level of bearing deterioration has increased and the time remaining is close to bearing collapse, the frequency is dominated by a frequency of 103.1 Hz as shown in Figure 5(b).

Table 1 provide an information related to the bearing fundamental frequencies. It is well known that if one or more frequencies from Table 1 appear in the FFT of the bearing vibration signal, this indicate that the bearing is in fault condition. In addition, each frequency listed in Table 1 correlate with one type of bearing fault condition. In low speed slew bearing, the bearing fault signal is buried in the background noise as presented in Figures 3-5. Thus none of the fundamental frequency presented in Table 1 appear in the FFT. The frequency of the bearing vibration signal were dominated by the frequency of 103 Hz, 131 Hz, 1356 Hz and

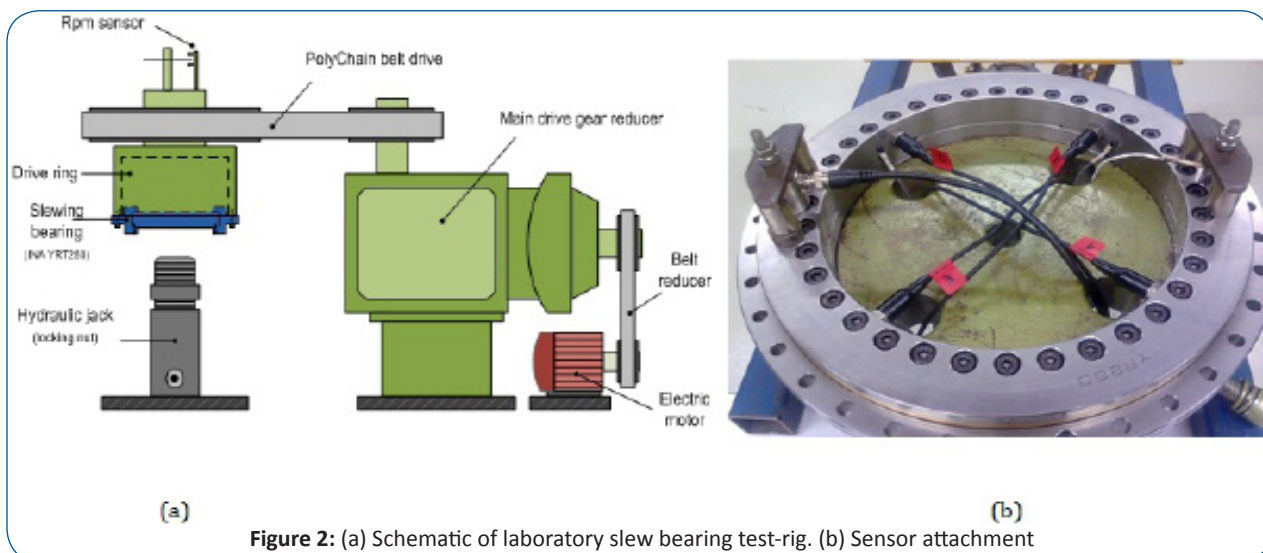


Figure 2: (a) Schematic of laboratory slew bearing test-rig. (b) Sensor attachment

Table 1: Fault frequencies of slew bearing run at 1 rpm [calculation is given in Appendix A]

Defect mode	Fault frequencies (Hz)	
	Axial	Radial
Outer ring (BPFO)	1.32	0.55
Inner ring (BPFI)	1.37	0.55
Rolling element (BSF)	0.43	0.54

1770 Hz.

According to the results, it can be concluded that the fault frequencies listed in Table 1 are difficult to identify using the FFT from the incipient defect (after dust insertion) to complete failure. One piece of information which can be identified from the raw vibration data is that the amplitude of the vibration signal increased gradually from February 24, May 3 to August 30 shown in Figures 3(a) – 5(a). As FFT-based vibration is not appropriate, the feature extraction method was then considered.

Previous Feature Extraction Study

Prior to the present study, some feature extraction methods have been employed and investigated [1, 2]. Caesarendra et al

[1] discusses the time domain features such as mean, variance, skewness and kurtosis extracted from raw vibration data, from empirical mode decomposition (EMD) and from wavelet packet decomposition. The features are compared to proposed circular domain features such as circular mean, circular variance, circular skewness and circular kurtosis extracted from processed vibration signal using piecewise aggregate approximation (PAA). The paper concludes that the features extracted from wavelet decomposition and the new circular domain features extracted from the PAA result are better than the features extracted from raw vibration data and EMD. In addition, the circular domain features and wavelet decomposition features are better at identifying the onset of a bearing condition but the progression of deterioration is not clearly visible. Caesarendra et al [2] presents four non-linear feature extraction methods, namely: the largest Lyapunov exponent, fractal dimension, correlation dimension and approximate entropy. Four non-linear features show the fluctuation in the last period of measurement, however the results are very noisy. The combined method between circular domain features with largest Lyapunov exponent algorithm is presented in [13]. The combined method produces the feature results better than features discussed in [2], however, the detection occurs too late. The fluctuation is detected in the very last measurement

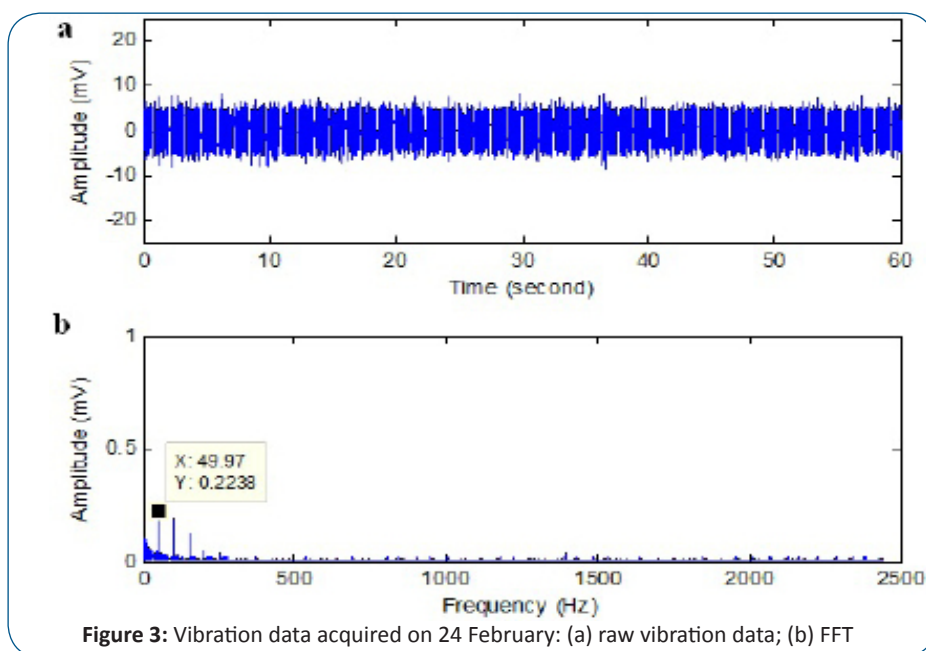


Figure 3: Vibration data acquired on 24 February: (a) raw vibration data; (b) FFT

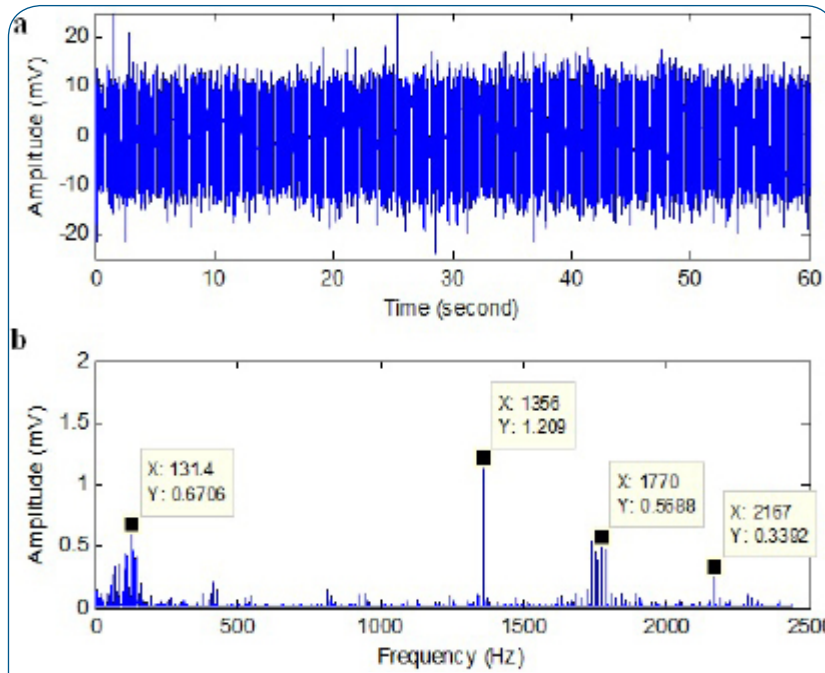


Figure 4: Vibration data acquired on 24 February: (a) raw vibration data; (b) FFT

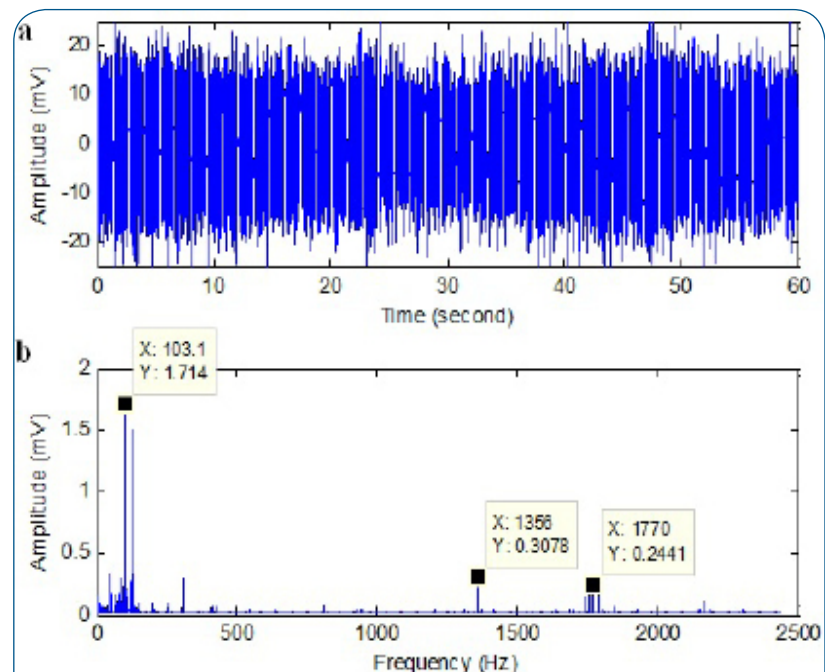


Figure 5: Vibration data acquired on 3 May: (a) raw vibration data; (b) FFT

period. If the maintenance workers rely on the result of [13], the maintenance scheduling will be missed and catastrophic failure may occur because there is not enough time for maintenance planning. Although the features obtained from previous studies have its own advantages, it must be improved in order to predict failure in a more timely fashion.

The RMS and kurtosis extracted from original vibration during 139 measurement days are presented in Figure 6.

Mathematical Morphology Operators as Feature Extraction Method of Vibration Signal

Because of the value of the MM method as shown in recent literature [9-12], this is the method selected in the present study as a non-linear signal processing or a non-linear signal reconstruction method. In this study, the six morphological operators: dilation, erosion, closing, opening, gradient 1 and

gradient 2 have been examined empirically with different SE numbers from 0.1T to 0.9T. The selected empirical results are shown in Appendix B. Four standard morphological operators (erosion, dilation, closing and opening) with two different SEs (0.1T and 0.9T) are presented in Tables 5 to 10 and for the result of gradient 1 and gradient 2 operator is presented in Tables 11 to 13. According the empirical results shows in Tables 5 to 10, the general conclusion can be made based on visual inspection as follows:

- (1) RMS and kurtosis of 0.9T structuring element (SE) are more noisy than RMS and kurtosis of 0.1T SE. These proofs that as SE increase the RMS and kurtosis feature are become less accurate.
- (2) RMS results extracted from four different MM operators and two other operators at BPFI, BPFO and BSF frequency are

Table 2: Pulse repetition period T for MM method

Type of pulse repetition period (T)	Axial	Radial
Outer race fault period (T_{BPFO})	$1/1.32 = 0.76$	$1/0.55 = 1.82$
Inner race fault period (T_{BPFI})	$1/1.37 = 0.73$	$1/0.55 = 1.82$
Ball fault period (T_{BSF})	$1/0.43 = 2.33$	$1/0.54 = 1.85$

Table 3: Summarised MATLAB script of Mathematical Morphology method as a feature extraction method for low speed slew bearing vibration monitoring

Proposed feature extraction method based on mathematical morphology operators (summarised MATLAB script)

1:	% Input the vibration data data = load('filename.txt');
2:	% Calculate the fault frequencies (the formula is given in Appendix A): BPFO = 1,32; BPFI = 1.37; BSF = 0.43;
3:	% Calculate the fault periods: $T_{BPFO} = 0.76$; $T_{BPFI} = 0.73$; $T_{BSF} = 2.33$;
4:	% Select the structuring element (SE) length. SE = 0.1~0.9:
5:	% Creating a new data input based on the selected SE length: X = SE*data;
6:	% Creating a structuring element data based on the new data X: SE_data = strel(ones(X,1));
7:	% Signal processing using basic MM operators: erosion = imerode(data, SE_data); % erosion signal processing dilation = imdilate(data, SE_data); % dilation signal processing closing = imerode(dilation, SE_data); % closing signal processing opening = imdilate(erosion, SE_data); % opening signal processing
8:	% Signal processing using gradient operators: gradient1 = data-erosion; % gradient1 signal processing gradient2 = dilation-data; % gradient2 signal processing
9:	% Calculating RMS feature from different proceed signals: RMS_erosion = sqrt(sum(erosion.^2)/size(erosion,1)); RMS_dilation = sqrt(sum(dilation.^2)/size(dilation,1)); RMS_closing = sqrt(sum(closing.^2)/size(closing,1)); RMS_opening = sqrt(sum(opening.^2)/size(opening,1)); RMS_gradient1 = sqrt(sum(gradient1.^2)/size(gradient1,1)); RMS_gradient2 = sqrt(sum(gradient2.^2)/size(gradient2,1));
10:	% Calculating kurtosis feature from different proceed signals: Kurtosis_erosion = kurtosis(erosion); Kurtosis_dilation = kurtosis(dilation); Kurtosis_closing = kurtosis(closing); Kurtosis_opening = kurtosis(opening); Kurtosis_gradient1 = kurtosis(gradient1); Kurtosis_gradient2 = kurtosis(gradient2);

identical to RMS extracted from original vibration data as presented in Figure 6(a). This result indicates that the MM method is hard to detect the degradation trend based on the three fault frequencies (BPFI, BPFO and BSF). Therefore, another frequency that is 103 Hz is also investigated in present study. This frequency is obtained from the FFT result as presented in Figure 5.

(3) Kurtosis results of four standard operators of MM method does not improve the kurtosis extracted from original vibration data as presented in Figure 6(b). In addition, kurtosis extracted from processed vibration signal using gradient 2 operator shows have some fluctuation in the last measurement day (approximately starts from day 100). It indicates that the bearing condition close to unpredicted

Table 4: Dimensions and properties of three-row slew bearing (axial/radial bearing INA YRT260)

Dimension or Property	Unit
Inner diameter (D_i)	260 mm
Outer diameter (D_o)	385 mm
Mass (m)	18.3 kg
Basic dynamic load rating (C)	109 kN (axial)
	102 kN (radial)
Basic static load rating (C_o)	810 kN (axial)
	310 kN (radial)
Number of rolling element (z)	161 (axial)
	66 (radial)
Diameter of rolling element (d_r)	6 mm (axial)
	5 mm (radial)
Pressure angel (α)	0° (axial)
	90° (radial)
Mean bearing diameter (d_m)	325.6 mm (axial)
	304 mm (radial)

failure. The selected kurtosis features of MM method are shown in Figure 7.

Based on the conclusion No.2, another RMS feature extracted from different processed signal is also investigated. The processed signal is obtained from similar six MM operators but with different SE. The SE used is one of dominant frequencies shows in Figure 5. The objective is to investigate the effect of dominant frequency appear in FFT result. The comparison of RMS results is presented in Figure 8. It can be seen that the RMS of SE = 1/103Hz is better than the RMS extracted from the original vibration signal and four standard MM operators in terms of the increasing value. In practice the increase number of RMS corresponds to the vibration level and the fault of bearing. The alert of bearing failure can be monitored and predicted.

In addition, a good MM results as the features can be obtained if the selected morphological operators and structuring element (SE) are appropriate. In this study the good MM result means that the features extracted from the processed signal show obvious deterioration of the bearing condition. This can be seen in Figures 7 and 8. Furthermore, as suggested in the literature, any of the four morphological operators can be used and some specific operators may be more useful for the signal being analyzed than others. The literature notes that the range of SE is usually from 0.1T to 0.9T, where T is the pulse repetition period. In this paper, T refers to the duration of bearing fault signals which is calculated from the fundamental fault frequencies of the slew bearing, as shown in Table 1. The calculation of T is

TABLE 5: RMS OF different MM OPERATORS AND DIFFERENT SES ($T = 1/BPFI$)

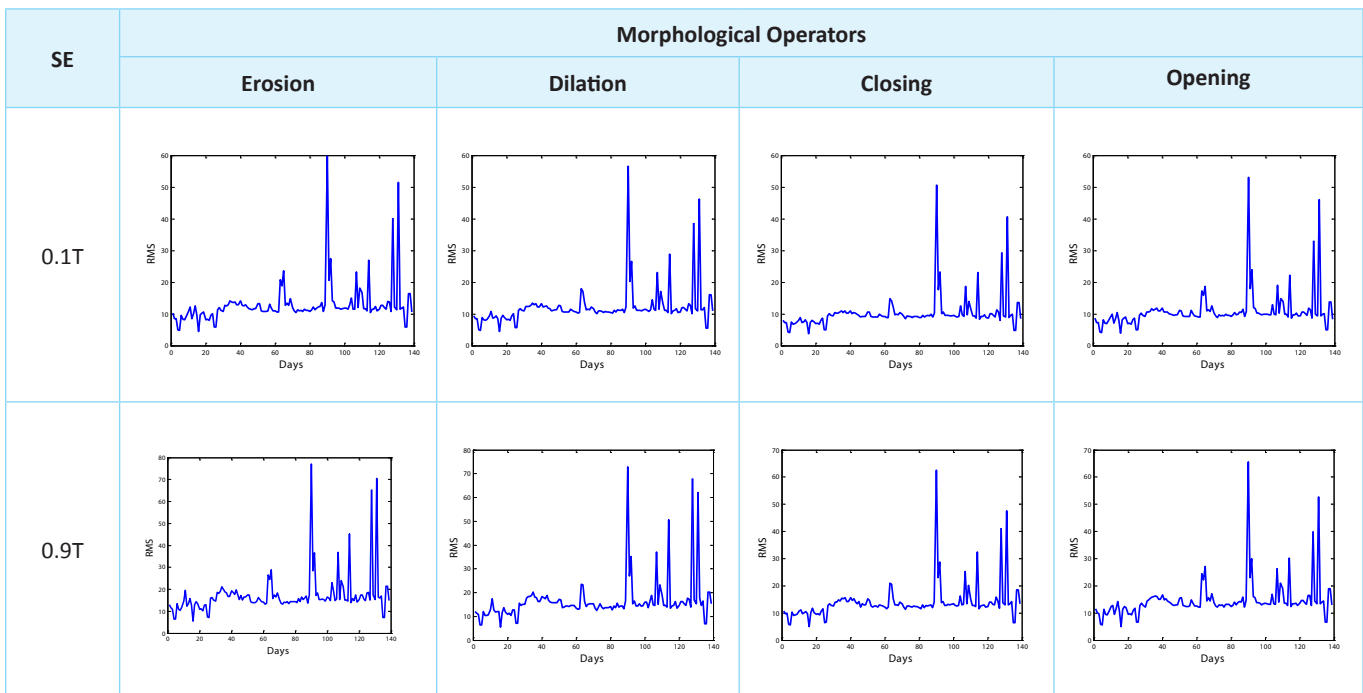


TABLE 6: KURTOSIS OF different MM OPERATORS AND DIFFERENT SES (T = 1/BPFI)

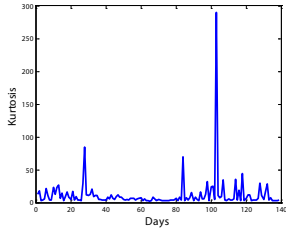
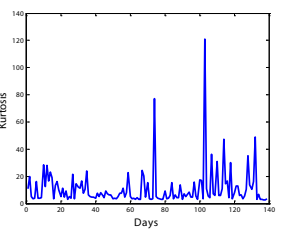
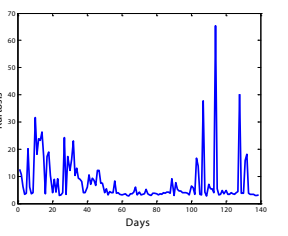
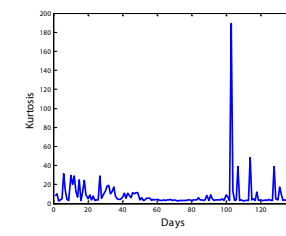
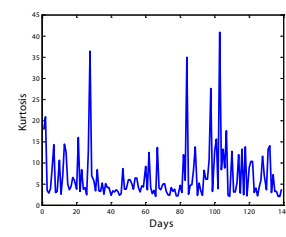
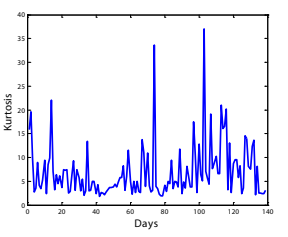
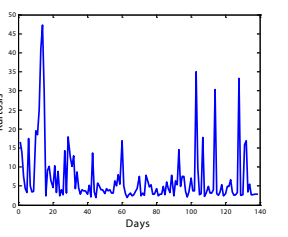
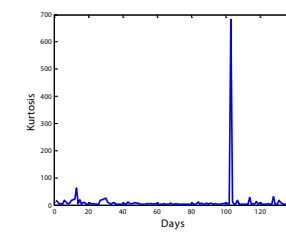
SE	Morphological Operators			
	Erosion	Dilation	Closing	Opening
0.1T				
0.9T				

TABLE 7: RMS OF different MM OPERATORS AND DIFFERENT SES (T = 1/BPFO)

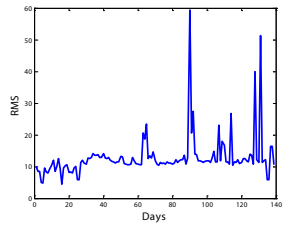
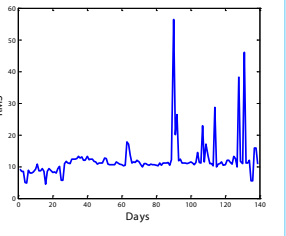
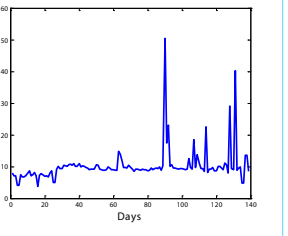
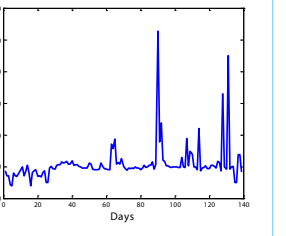
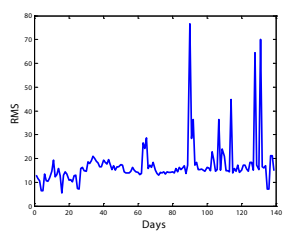
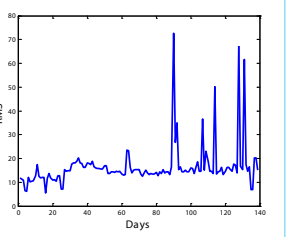
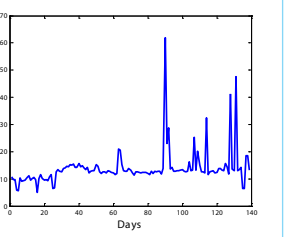
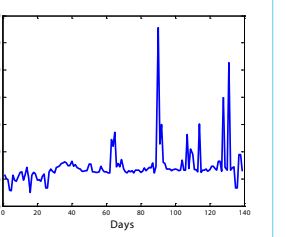
SE	Morphological Operators			
	Erosion	Dilation	Closing	Opening
0.1T				
0.9T				

TABLE 8: KURTOSIS OF different MM OPERATORS AND DIFFERENT SES (T = 1/BPFO)

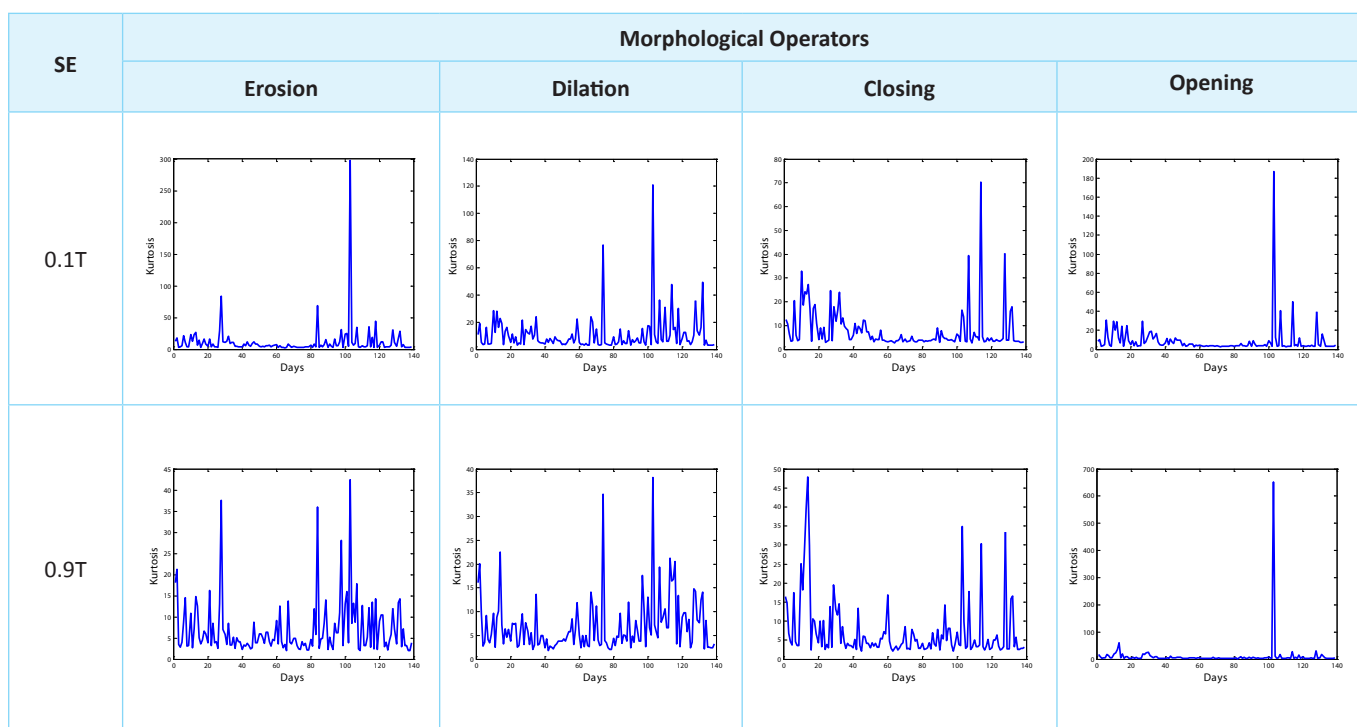


TABLE 9: RMS OF different MM OPERATORS AND DIFFERENT SES (T = 1/BSF)

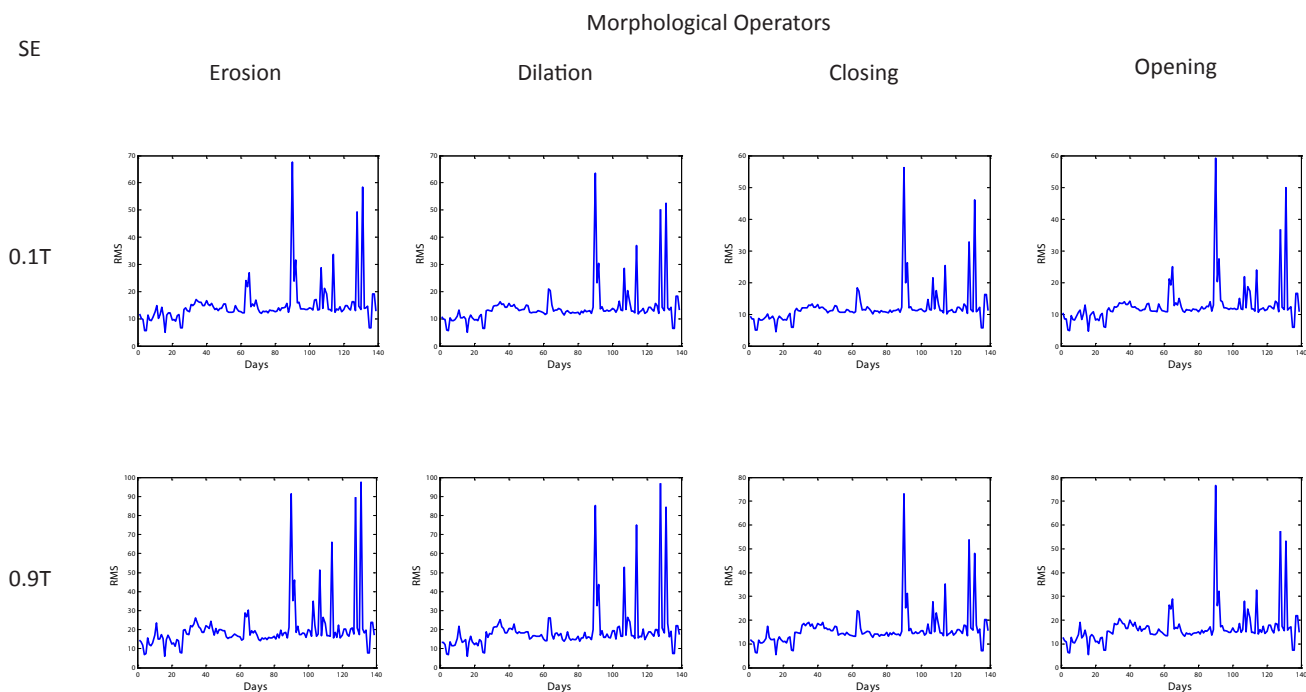


TABLE 10: KURTOSIS OF different MM OPERATORS AND DIFFERENT SES (T = 1/BSF)

SE	Morphological Operators			
	Erosion	Dilation	Closing	Opening
0.1T				
0.9T				

TABLE 11: RMS AND KURTOSIS OF DIFFERENT GRADIENT OPERATORS AND DIFFERENT SES (T = 1/BPFI)

SE	Morphological Operators			
	Gradient 1	Gradient 2	Gradient 1	Gradient 2
	RMS	RMS	Kurtosis	Kurtosis
0.1T				
0.9T				

TABLE 12: RMS AND KURTOSIS OF different GRADIENT OPERATORS AND DIFFERENT SES ($T = 1/BSFO$)

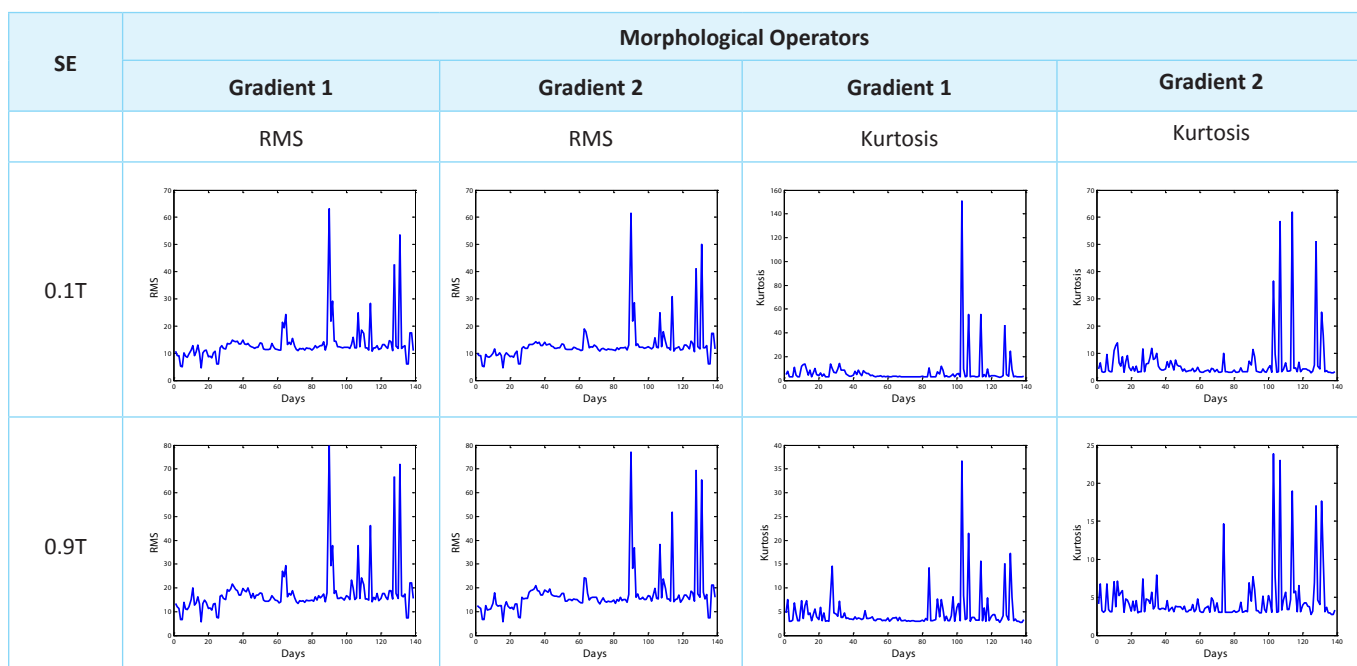
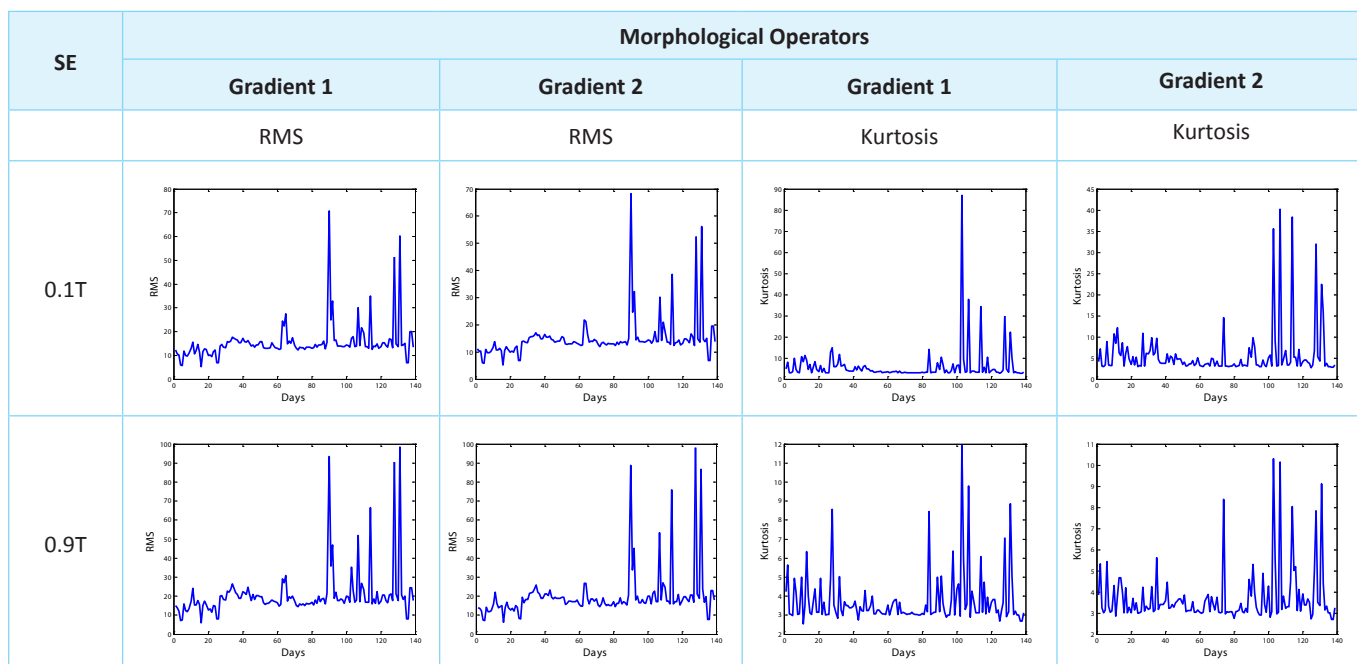


TABLE 13: RMS AND KURTOSIS OF different GRADIENT OPERATORS AND DIFFERENT SES ($T = 1/BSF$)



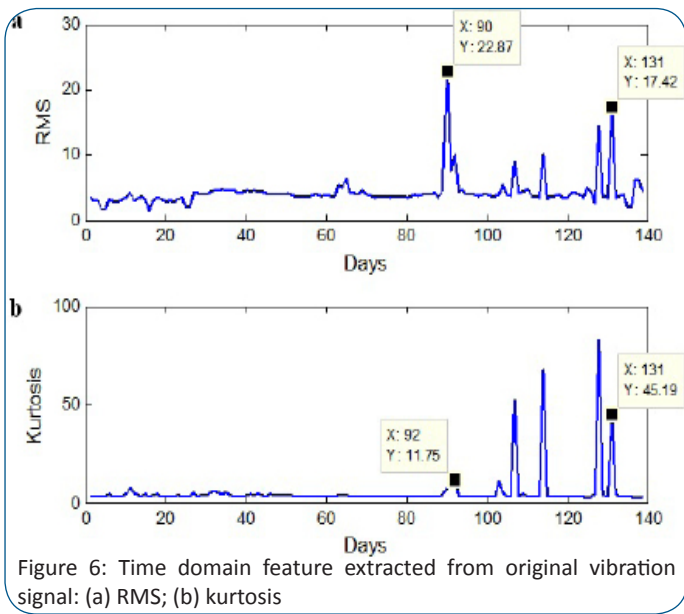


Figure 6: Time domain feature extracted from original vibration signal: (a) RMS; (b) kurtosis

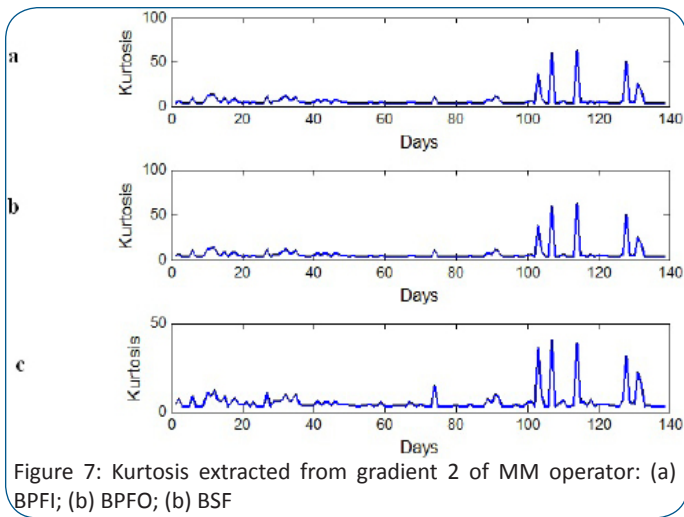


Figure 7: Kurtosis extracted from gradient 2 of MM operator: (a) BPF1; (b) BPF0; (c) BSF

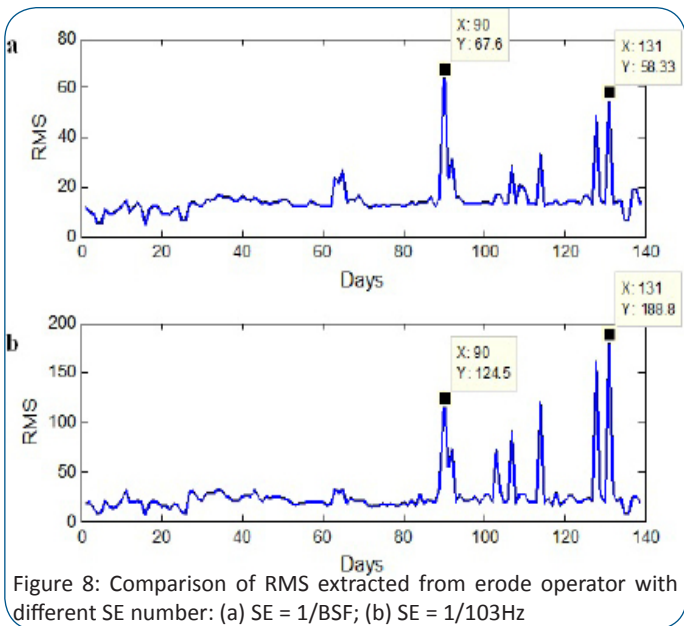


Figure 8: Comparison of RMS extracted from erode operator with different SE number: (a) SE = 1/BSF; (b) SE = 1/103Hz

presented in Table 2. We selected the fault frequencies in the axial direction because the load in the laboratory slew bearing test rig is applied in the axial direction. Thus, the raceway of the axial direction of the slew bearing has a greater possibility of failure than that of the radial direction.

Slew Bearing Damage

During the slew bearing lab experiment, complete failure is unpredictable. A sudden burst vibration signal occurred on September 2nd 2007 and the test-rig had to be shut down. To be able to discover the severe damage to the slewing bearing and clarify the result of the feature calculation, the slewing bearing was dismantled for inspection after the test-rig was shut down on day 139. Some of the defective regions can be clearly seen in Figure 9.

Conclusions

A new application of the non-linear signal processing method based on the mathematical morphology (MM) method has been presented. The application of MM operators in the slew bearing vibration signal can improve RMS and kurtosis feature which provides a more accurate picture of bearing deterioration. The RMS extracted from processed vibration signal using erode and gradient 1 operator is better than RMS extracted from original vibration signal; and the kurtosis of processed vibration signal using gradient 2 operator is better than kurtosis extracted from original vibration signal. In vibration analysis, MM offers the solution to geometry-based problems especially to quantify the shape and the size of the signals, which cannot be done with the traditional tools of the linear system or Fourier analysis. This shows that the MM result improves the time domain features of the original vibration signal for low speed slew bearings.

Acknowledgments

The first author thanks the University of Wollongong for the financial support through University Postgraduate Award (UPA) and International Postgraduate Tuition Award (IPTA) during this study. The authors gratefully acknowledge the help of Dr. Madeleine Strong Cincotta in the final language editing of this paper.

Appendix A: Bearing fault frequency formula [15]

- Fault frequency of outer ring:

$$F_{OR} = \left| \frac{IR_{rpm} - OR_{rpm}}{2} \right| \cdot \left[1 - \frac{(\cos(\alpha)) \cdot d_r}{d_m} \right] \cdot z \quad (A1)$$
- Fault frequency of inner ring:

$$F_{IR} = \left| \frac{IR_{rpm} - OR_{rpm}}{2} \right| \cdot \left[1 + \frac{(\cos(\alpha)) \cdot d_r}{d_m} \right] \cdot z \quad (A1)$$
- Fault frequency of rolling element:

$$F_R = \left| \frac{IR_{rpm} - OR_{rpm}}{2} \right| \cdot \left[\frac{d_m}{d_r} - \frac{(\cos(\alpha))^2 \cdot d_r}{d_m} \right] \cdot z \quad (A1)$$

where IR_{rpm} and OR_{rpm} are the rotational speed of the inner ring and outer ring respectively. For 1 rpm the value of IR_{rpm} is 1 and the value of OR_{rpm} is 0. d_m is the mean bearing diameter, d_r is diameter of the rolling element, and z is number of rolling

elements. (A1), (A2) and (A3) can be calculated using the properties and dimension presented in Table 4.

Appendix B: Feature Extraction Results based on Mathematical Morphology Operators.

References

1. Caesarendra W, Kosasih B, Tieu AK, Moodie CAS. Circular domain features based condition monitoring for low speed slewing bearing. *Mechanical Systems and Signal Processing*. 2014; 45(1): 114-138. doi:10.1016/j.ymssp.2013.10.021.
2. Caesarendra W, Kosasih B, Tieu K, Moodie CAS. An application of nonlinear feature extraction – A case study for low speed slewing bearing condition monitoring and prognosis. *Proceeding of the 12th IEEE/ASME International Conference on Advanced Intelligent Mechatronics (AIM)*; 2013 July 9-12; Wollongong, Australia. p. 1713-1718.
3. Serra J. *Image analysis and mathematical morphology*. New York: Academic Press; 1982.
4. Nishida S, Nakamura M, Miyazaki M, Suwazono S, Honda M, Nagamine T, et al. Construction of a morphological filter for detecting an event related potential P300 in single sweep EEG record in children. *Medical Engineering Physics*. 1995; 17(6): 425-430.
5. Nishida S, Nakamura M, Shindo K, Kanda M, Shibasaki H. A morphological filter for extracting waveform characteristics of single sweep evoked potentials. *Automatica*. 1997; 35: 937-943. doi:10.1016/S0005-1098(98)00230-1.
6. Nishida S, Nakamura M, Ikeda A, Shibasaki H. Signal separation of background EEG and spike by using morphological filter. *Medical Engineering Physics*. 1999; 21(9): 601-608.
7. Sedaaghi MH. ECG wave detection using morphological filters. *Applied Signal Processing*. 1998; 5: 182-194.
8. Nikolaou NG, Antoniadis IA. Application of morphological operators as enveloped extractors for impulsive-type periodic signals. *Mechanical Systems and Signal Processing*. 2003; 17(6): 1147-1162. doi:10.1006/mssp.2002.1576.
9. Zhang L, Xu J, Yang J, Yang D, Wang D. Multiscale morphology analysis and its application to fault diagnosis. *Mechanical Systems and Signal Processing*. 2008; 22(3): 597-610. doi:10.1016/j.ymssp.2007.09.010.
10. Wang J, Xu G, Zhang Q, Liang L. Application of improved morphological filter to the extraction of impulsive attenuation signals. *Mechanical Systems and Signal Processing*. 2009; 23(1): 236-245. doi:10.1016/j.ymssp.2008.03.012.
11. Dong Y, Liao M, Zhang X, Wang F. Fault diagnosis of rolling element bearings based on modified morphological method. *Mechanical Systems and Signal Processing*. 2011; 25(4): 1276-1286. doi:10.1016/j.ymssp.2010.10.008.
12. Santhana Raj A, Murali N. Early classification of bearing faults using morphological operators and fuzzy inference. *IEEE Transactions on Industrial Electronics*. 2013; 60(2): 567-574. doi: 10.1109/TIE.2012.2188259.
13. Caesarendra W, Kosasih B, Tieu AK, Moodie CAS. Condition monitoring of low speed slewing bearing based on largest Lyapunov exponent algorithm and circular-domain feature extractions. *Proceeding on 26th International Congress of Condition Monitoring and Diagnostic Engineering Management*; 2013 June 11-13; Helsinki, Finland.
14. Moodie CAS. *An Investigation into the Condition Monitoring of Large Slow Speed Slew Bearings*. Ph.D. thesis, University of Wollongong, Wollongong, 2009.
15. Eschmann P, Hasbargen L, Weigand K. *Die Wälzlagerpraxis: Handbuch für die Berechnung und Gestaltung von Lagerungen*. München: R. Oldenburg; 1953.